

On Quadruped Attitude Dynamics and Control Using Reaction Wheels and Tails

Konstantinos Machairas and Evangelos Papadopoulos

Abstract— This paper studies the attitude dynamics and the control of quadruped robots using tail-like appendages during the flight phases of high speed locomotion. Inspiration and data are first obtained from cheetah’s fast galloping techniques. A two-body template is then used to simply describe the dynamics of a large body whose attitude is controlled by a rotating appendage. The equations of motion for a tail and a reaction wheel are given, while by employing cyclic coordinates, all possible reductions are performed to finally lead to the design of model-based controllers. A main contribution lies on the thorough discussion on the holonomy of the system, which only depends on the system’s geometry and the initial angular momentum. A comparison between a reaction wheel and a tail is also carried out, while basic steps and formulas are proposed for selecting the key parameters concerning the design of such systems. Finally, simulation results are presented in order to validate the methods proposed herein.

I. INTRODUCTION

Quadruped robots are highly underactuated machines, while most of their tasks, such as high speed galloping, jumping over obstacles, or gait transitions, require precise control of their attitude. Although much research has been conducted concerning the control of legs of different morphologies, attitude control of the body is yet poorly investigated. So far, attitude control is mostly achieved indirectly through the motion of the legs, a technique that assigns more control tasks to the legs forcing them to trade-offs that may lead to low performance. To better mitigate this challenge, dedicated appendages with large moment of inertia (MoI) can be used.

Once again, ideas can be derived from biology; one quickly thinks of animal tails. The impressively rich repertoire of the mammalian tail’s functions has been well reviewed in [1]. As discussed in detail, it is a multifunctional appendage that is important in swimming, crawling, running, digging, climbing, gliding, and flying, while it is also used as a prop to rest, a weapon, a protective barrier, or even a mechanism for thermoregulation. Interestingly, it has been reported that the portion of the brain of the spider monkey

responsible for control of the tail is even larger than that for the control of the hind limb.

Regarding balance, the tail may assume the functions of counter-balance, prop or rudder. Many of the quadruped mammals have long tails which aid in balance and maneuverability at high speeds. Kangaroo rats use their long tails for righting and turning in midair, while black rats are able to enter a building by balancing along a 2 mm wire. Studying hopping by kangaroos, we observe the two legs moving in phase tending to make the rest of the body pitch. However, as reported in [2], appropriate tail movements reduce this effect. To sum up, for most legged animals, tail movements are effective for adjustments to unexpected perturbations, when the legs are otherwise occupied.

In [3] a general conclusion can be derived when studying dog’s locomotion. It is reported that without a mechanism for balance, any step involving a net fore-aft acceleration also involves a nose-up or nose-down pitching of the body. This mechanism can be a lizard’s tail, a cheetah’s torso or even a human’s arms. A cheetah though may not rely on its tail to be the fastest animal on earth, but a human strongly relies on his arms to run faster and more efficiently, [4]. In fact, humans can also run with the hands on their pockets, but by swinging them they better regulate their gait and stabilize their motion.

Although numerous legged robots have been designed, only a minority of them includes appendages for angular momentum management, such as tails or reaction wheels. The first legged robots that used a tail were the Uniuro, [5], and the TITRUS-II, [6]. In [7] a bio-inspired robot was developed to investigate the effectiveness of a tail in 3D attitude control, while in [8] Tailbot and XRL used a tail for self-righting. TAYLRoACH was able to make rapid precise turns, [9], and FlipBot was able to perform a 360° roll rotation in under a second using its lizard-inspired tail, [10]. A tail was used in a planar hopping robot to inject energy in the leg spring, [11], while a tail-like appendage was used to improve stability of a quadruped robot, [12]. Furthermore, the biped robot Zappa was able to walk with only one actuator moving its tail, [13], and the climbing robot ROCR used a tail to propel itself upward, [14].

A number of studies have also dealt with attitude control under conservation of angular momentum, and methods that can lead a mechanism to a desired final configuration from an initial given one have been developed, [15-18]. However, in literature, only a couple of studies include comparisons of reaction wheels and tails, [19, 20]. Although tails are mostly used in legged locomotion, the topic remains open, since

Acknowledgment. This research has been financed by the European Union (European Social Fund – ESF) and Greek national funds through the Operational Program “Education and Lifelong Learning” of the National Strategic Reference Framework (NSRF) – Research Funding Program: ARISTEIA: Reinforcement of the interdisciplinary and/ or inter-institutional research and innovation.

K. Machairas and E. Papadopoulos (e-mail: {kmach, egpapado}@central.ntua.gr), are with the Department of Mechanical Engineering, National Technical University of Athens, 15780 Athens, Greece.

there are also several robots using reaction wheels, [21-23], including one of the fastest legged robots ever built, [24].

In this work, we present an analysis on the attitude dynamics and the pitch control of quadruped robots using dedicated tail-like appendages. First, useful data are obtained from cheetah's fast galloping techniques. Second, a simple planar template of two coupled bodies is introduced in order to perform the analysis on the simplest dynamics possible, and to go into a thorough discussion about the system's holonomy, which is one of the main contributions of this paper. Then, after all possible reductions are performed on the dynamics, model-based controllers are designed, and key steps and formulas are proposed concerning the design of robots that use reaction wheels and tails. Simulations are carried out regarding robot maneuvers using a reaction wheel and a tail, and useful conclusions are derived by comparing the two appendages.

II. OBSERVATIONS FROM NATURE

One can make several useful observations trying to unveil the secrets behind the incredible performance of the fastest animal on earth, the cheetah. Snapshots from the video in [25] are presented in Fig. 1, to help the analysis. Obviously, attitude control of the body is an important aspect of the rotary gallop gait that the cheetah uses to reach its full speed. This is an asymmetrical gait, where the feet fall in a circular sequence around the body, and includes two flight phases: a gathered one, where the torso is flexed and the hind legs pass in front of the fore legs, and an extended one, where the torso is extended and all legs are stretched away from the body, see Fig. 1. It is yet a fact that the cheetah does not rely mainly on its tail to completely control its pitch angle, but rather it uses it for fine adjustments of its attitude. However, trying to extract indicative values for later use, it is useful to study the attitude of the cheetah's body during a stride.

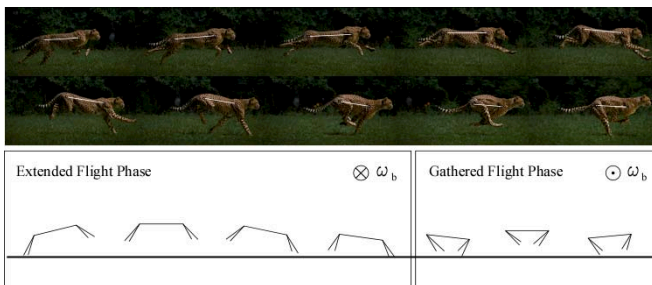


Figure 1. Snapshots from the video in [25], showing a cheetah galloping.

To this end, putting aside the complex motion of the torso and focusing on the line connecting the fore and the hind hip, we make a first estimation of how the cheetah manages its body angular momentum in order to best position its legs in every touchdown. We notice a cyclic change of positive and negative angular momentum; during the extended flight phase, after hind legs push the ground, the body gets positive initial angular momentum, while in the gathered flight phase, after fore legs push the ground the body gets negative initial angular momentum. The body pitching along with the

duration of the two phases are calculated and listed in Table I. These observations provide indicative values for the analysis presented herein.

TABLE I. CHEETAH'S LOCOMOTION DATA

Time (s)	Body Pitch Angle (Degrees)	Phase
0.48	4.9	Extended Flight Phase $\Delta t = 0.08$ s $\Delta\theta = -14^\circ = -0.244$ rad $\omega = \Delta\theta/\Delta t = -3.05$ rad/s
0.5	2.5	
0.52	-0.1	
0.54	-5.4	
0.56	-9.1	Gathered Flight Phase $\Delta t = 0.06$ s $\Delta\theta = 6.3^\circ = 0.110$ rad $\omega = \Delta\theta/\Delta t = 1.83$ rad/s
0.63	-9	
0.66	-4.5	
0.69	-2.7	
-	-	

III. ROBOT DYNAMICS AND ANGULAR MOMENTUM

A. Model and Dynamics

To study the effects of a moving appendage on a body in ballistic flight, we introduce a simple planar template of two coupled bodies, see Fig. 2. We make this severe assumption (rigid spine and massless legs) on purpose, in order to perform the analysis on the simplest dynamics possible, and to go into a discussion about holonomy that would not be possible with more complex models. Hereafter, by body we mean the body along with all other links of a quadruped, except for the tail, which here plays the role of a general angular momentum control device; a reaction wheel is also covered by this analysis.

First, we parameterize the system's configuration space by the absolute pitch angle of the body $\theta \in S^1$, the relative hinge angle of the tail $q \in S^1$, and the position vector $p \in R^2$ of the system center of mass (CoM) in the inertial reference frame, yielding the space $Q = S^1 \times S^1 \times R^2$. Let (m_0, I_0) and (m_1, I_1) denote the pairs of mass and MoI of the body and the tail about their CoM. Let also r be the distance from the body's CoM to the joint, and l be the distance from the tail's CoM to the joint, see Fig. 2. Finally, let τ be the control torque that the body exerts on the tail.

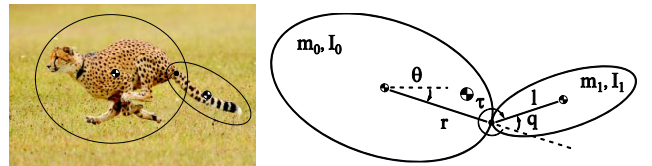


Figure 2. A cheetah during flight phase, and the two-body template.

A reduction to the system's CoM frame is now possible, since the uniform gravitational field allows the separation of the CoM motion from the relative motion dynamics; the system's CoM behaves as a single particle under the action of external gravitational forces. The reduced configuration manifold is now $Q' = S^1 \times S^1$, parameterized by the generalized coordinates θ and q , and the Lagrangian is equal to the kinetic energy since gravitational forces are no more considered.

$$L = \frac{1}{2}\mu((l^2+r^2+2rl\cos q)\dot{\theta}^2+l^2\dot{q}^2+2(l^2+rl\cos q)\dot{q}\dot{\theta}) + \frac{1}{2}I_0\dot{\theta}^2 + \frac{1}{2}I_1(\dot{\theta}^2+\dot{q}^2+2\dot{q}\dot{\theta}) \quad (1)$$

We note that the masses appear only in the form of an important quantity $\mu=(m_1m_2)/(m_1+m_2)$ that we can call the system's effective mass. The equations of motion (EoM) can now be derived using the Lagrange formulation, to yield:

$$(I_0+I_1+\mu(l^2+r^2+2rl\cos q))\ddot{\theta}+(I_1+\mu(l^2+rl\cos q))\ddot{q}-\mu rl\sin q\dot{q}^2-2\mu rl\sin q\dot{q}\dot{\theta}=0 \quad (2)$$

$$(I_1+\mu l^2+\mu rl\cos q)\dot{\theta}+(I_1+\mu l^2)\dot{q}+\mu rl\sin q\dot{\theta}^2=\tau$$

B. Angular Momentum

An attempt is made to express the EoM in the simplest form possible, using the conservation of angular momentum. In general, if a conservation law exists, the Lagrangian provides the integral of motion as an equation of motion. We first note that the generalized coordinate θ does not appear in the Lagrangian, and that makes it a cyclic or ignorable coordinate. Coordinate q , which does appear in the Lagrangian, is called palpable or positional. As a result the generalized momentum associated to the cyclic coordinate is conserved ($\partial L / \partial \dot{\theta} = \text{const}$) yielding:

$$(I_0+I_1+\mu(l^2+r^2+2rl\cos q))\dot{\theta}+(I_1+\mu(l^2+rl\cos q))\dot{q}=h_0 \quad (3)$$

which is in fact the conservation of the system's angular momentum equation about the system's CoM. Equation (3) is an integral of motion and the constant of motion h_0 is the system's initial angular momentum. Since an integral of motion exists, one of the EoM equations can be substituted with the first order conservation equation resulting in a set of a second-order and a first-order differential equation.

C. Integrability of the Constraint – Analytical Results

A question now arises about whether one can integrate the angular momentum equation to derive a useful analytical expression between the body angle θ and the hinge angle q . In general, a constraint that can only be expressed by the differential of the configuration space coordinates and time is a nonholonomic constraint; else if the differential constraint can be integrated, it is in fact a holonomic constraint in disguise. A distinction should also be made between dynamic nonholonomic constraints, i.e. constraints that are not externally imposed on the system, but rather are consequences of the EoM and practically equations of conservation laws, and kinematic nonholonomic constraints, i.e., constraints imposed by the kinematics, such as rolling, [27]. Obviously, the conservation of angular momentum is a dynamic constraint and can take the form of an acatastatic Pfaffian constraint, ($\cos q = cq$):

$$(I_0+I_1+\mu(l^2+r^2+2rl\cos q))d\theta+(I_1+\mu(l^2+rl\cos q))dq=h_0dt \quad (4)$$

$$\text{or} \quad P(q)d\theta+Q(q)dq+Rdt=0 \quad (5)$$

The necessary and sufficient condition for (5) to have an integrating factor and therefore to be integrable is, [26]:

$$I = P\left(\frac{\partial Q}{\partial t} - \frac{\partial R}{\partial q}\right) + Q\left(\frac{\partial R}{\partial \theta} - \frac{\partial P}{\partial t}\right) + R\left(\frac{\partial P}{\partial q} - \frac{\partial Q}{\partial \theta}\right) = 0 \quad (6)$$

which yields:

$$h_0rl\sin q = 0 \quad (7)$$

Clearly, the constraint is integrable in most of the cases; it cannot be integrated analytically only when $r, l, h_0 \neq 0$, i.e. when the joint position does not coincide with either the body's or the appendage's CoM, and the system also starts the flight phase with nonzero angular momentum. The analytical derivations for all the integrable cases are useful, and therefore they are given below.

1. Zero Initial Angular Momentum

In this case, the conservation equation is integrable for every geometry. Integrating (4) with $h_0 = 0$ yields:

$$\theta = \theta_0 - \frac{1}{2}(q - q_0) - \frac{A}{C}\tan^{-1}\left(\frac{B}{C}\tan\frac{q}{2}\right) + \frac{A}{C}\tan^{-1}\left(\frac{B}{C}\tan\frac{q_0}{2}\right) \quad (8)$$

$$\text{where} \quad A = I_1 + \mu l^2 - I_0 - \mu r^2, \quad B = I_0 + I_1 + \mu(l - r)^2$$

$$C = \sqrt{(I_0 + I_1 + \mu l^2 + \mu r^2)^2 - (2\mu rl)^2}$$

This is a rather involved expression that gets much simpler when $r=0$ (the appendage is hinged at the body's CoM), or $l=0$ (the appendage rotates about its CoM).

2. Nonzero Initial Angular Momentum

In this case, integrability depends on the system's geometry.

a. If a tail is hinged at the body's CoM, then integrating (4) with $r=0$ yields:

$$(I_0+I_1+\mu l^2)(\theta-\theta_0)+(I_1+\mu l^2)(q-q_0)=h_0(t-t_0) \quad (9)$$

b. If a reaction wheel is hinged at distance r from the body's CoM, then integrating (4) with $l=0$ yields:

$$(I_0+I_1+\mu r^2)(\theta-\theta_0)+I_1(q-q_0)=h_0(t-t_0) \quad (10)$$

c. Finally, if a reaction wheel is hinged at the body's CoM (also known as "Elroy's Beanie", [27]), then integrating (4) with ($r=l=0$) yields the simplest expression:

$$(I_0+I_1)(\theta-\theta_0)+I_1(q-q_0)=h_0(t-t_0) \quad (11)$$

To sum up, if the appendage is a reaction wheel, the constraint is integrable – and therefore holonomic – with or without initial angular momentum. If the appendage is a tail, the constraint is integrable for any geometry when the initial angular momentum is zero. However, when the initial angular momentum is nonzero, the constraint is integrable only if the tail is hinged at body's CoM.

D. Discussion on the System's Holonomy

The restrictions on the motion of the system in the two cases – holonomic (or integrable) and nonholonomic (or nonintegrable) – are of different nature. In the holonomic case the constraint is geometric, i.e. the configuration of the system is actually constrained to be on a submanifold of the configuration manifold. In the nonholonomic case the constraint does not restrict θ and q , yet it restricts the direction of the path through a configuration (θ, q); at every configuration a constraint on velocities must be satisfied.

In conclusion, when conservation of angular momentum imposes a holonomic constraint on the system, the dimension of the accessible configurations' space is reduced; a body pitch angle θ corresponds to a single tail angle q . When the constraint due to the conservation of angular momentum is nonholonomic, the whole configuration manifold is accessible and any pair (θ, q) can be achieved. However, this constraint restricts the velocities at every point on the configuration manifold, and thus the state of the system depends on the path taken.

E. Discussion on Time Invariance

When initial angular momentum is zero, the constraint, which is holonomic for every geometry, is always scleronomic, i.e. time invariant – see (8). In those cases when initial angular momentum is nonzero and the system is also holonomic, the constraint depends on time, and thus it is a rheonomic constraint – see (9). This is in fact a time varying geometric constraint that binds the configuration coordinates. A practical explanation is that due to initial angular momentum the system experiences a steady drift in addition to the motions caused by the internal shape changes. If we fix the shape variable q , this drift will manifest itself as a steady angular rotation of the body with speed proportional to the initial angular momentum.

IV. MOMENTUM DEVICE DESIGN

Based on the analytical expressions derived above, we propose basic steps and formulas for the design of tail-like systems for legged robots. We consider here the length/ the radius and the mass of the tail or the wheel as the key design parameters. To this end, we first assume that the appendages are pinned at the body's CoM, since the EoM can be written decoupled in this case. Although hinge position is in general at a distance r from body's CoM, this assumption simplifies the expressions without bringing important deviations for alternative geometries.

A. Reaction Wheel Design

1. Given the desired time t and the desired body angle $\Delta\theta$, we derive an expression for the torque τ needed to achieve the maneuver, employing a simple bang-bang controller. This is the case where constant maximum torque accelerates the appendage for $t/2$, and the opposite torque is applied to decelerate it. Integrating twice the decoupled EoM for θ , and considering $\dot{\theta}_0=0$, yields:

$$I_0\ddot{\theta}=-\tau \Rightarrow \tau=-\frac{4I_0\Delta\theta}{t^2} \quad (12)$$

2. Given the calculated torque τ and the desired time t we derive an expression between the motor's angular velocity \dot{q} and the wheel's MoI I_l (we assume the reaction wheel carries all of its mass in its circumference i.e. $I_1=m_l\rho^2$). Integrating once the decoupled EoM for q , yields:

$$\frac{I_0I_1}{I_0+I_1}\dot{q}=\tau \Rightarrow \dot{q}=\frac{\tau t}{2}\left(\frac{1}{I_1}+\frac{1}{I_0}\right) \quad (13)$$

Varying I_l , and that is varying $m_l\rho^2$ (let ρ be the radius of the reaction wheel), we can find a suitable value for the maximum velocity of the wheel which is a key parameter for the selection of the motor. Note that for larger I_l , the angular velocity drops, while the radius ρ has a maximum value depending on the size of the robot's body.

B. Tail Design

1. Similarly to the wheel case, given the desired t and $\Delta\theta$ we estimate the torque τ needed for the maneuver using (12).

2. The tail case introduces an important restriction in the design process, i.e. q needs to be bounded since full rotation about the hinge is mechanically forbidden. Hence, starting from the bounds of the tail angle q , we aim to find values for the mass and the length of the tail that permit a desired maneuver $\Delta\theta$. In the holonomic and scleronomic cases, conservation of angular momentum shows how the mechanical properties of the body and the tail connect a $\Delta\theta$ rotation to a specific Δq one. Thus, regardless of the time needed, which in fact depends on the torque exerted, a desired connection of Δq and $\Delta\theta$ requires an equation of the system's mechanical properties to be satisfied, leading to an expression for the tail's mass calculation. For $I_1=0$, and $h_0=0$, (4) yields:

$$(I_0+\mu l^2)\Delta\theta+\mu l^2\Delta q=0 \Rightarrow m_l=\frac{-\Delta\theta I_0 m_0}{(\Delta\theta+\Delta q)l^2 m_0+\Delta\theta I_0} \quad (14)$$

A constraint for l being smaller than robot's height must be also considered. We also note that if $r \neq 0$ (which better reflects reality), this mass could be even smaller by a factor that would depend on r , due to the torque produced by the force exerted on the hinge.

3. Similarly to the wheel case, we derive an expression for the motor's maximum angular velocity by integrating once the decoupled EoM for q :

$$\frac{I_0\mu l^2}{I_0+\mu l^2}(\dot{q}-\dot{q}_0)=\tau t \Rightarrow \dot{q}=\frac{I_0+\mu l^2}{2I_0\mu l^2}\tau t \quad (15)$$

V. CONTROL

As discussed above, a quadruped robot needs to successfully control its attitude in order to run, jump, react to disturbances or perform other sophisticated tasks. Here, we assume that a simple controller that drives the body pitch angle θ to a desired value in time is sufficient for these tasks. Moreover, the tail angle q needs to be directly or indirectly controlled when designing a controller. Being difficult to control both θ and q with a single control input τ , we develop model-based controllers to control θ when we need to control the body attitude, and q when we need to position the tail to a desired angle.

A. Control of the Tail Angle q

Here, we focus on the system's dynamics to perform an extra reduction of the configuration space to the shape space (S^1), parameterized by the hinge angle q . To this end, we form the Routhian, $R=L-h_0\dot{q}$, which can be treated just like

a Lagrangian with $N-1$ degrees of freedom. Lagrange's equation for the palpable coordinate q yields the reduced dynamics in the form of a single equation:

$$D(q)\ddot{q}+C(q,\dot{q})\dot{q}+G(q,h_0^2)=\tau \quad (16)$$

Using (18) the following feedback linearization control scheme can be applied in order to control the tail angle q :

$$\tau=D(q)(\ddot{q}_d+k_v\dot{e}_q+k_p e_q)+C(q,\dot{q})\dot{q}+G(q,h_0^2) \quad (17)$$

Trajectory planning is implemented with a 5th degree polynomial, while k_v, k_p depend on the maneuver's duration.

B. Control of the Unactuated Body Angle θ

In order to control θ one should eliminate \ddot{q} from the second EoM (2), yielding a single equation of the form:

$$D^*(q)\ddot{\theta}+C^*(q,\dot{q},\dot{\theta})=\tau \quad (18)$$

A model-based controller is again applied to control θ , while trajectory planning is implemented similarly to (19).

$$\tau=D^*(q)(\ddot{\theta}_d+k_v\dot{e}_\theta+k_p e_\theta)+C^*(q,\dot{q},\dot{\theta}) \quad (19)$$

C. Stability of the Internal Dynamics

By the time the body pitch angle θ reaches the desired value, the system's stability depends on the stability of the internal dynamics, i.e. the stability of q . For zero initial angular momentum, when the body reaches the desired attitude, the tail also stops moving. However, for nonzero initial angular momentum, when the body stops, the tail has to keep rotating so that the system's angular momentum is kept constant. When the body angular velocity $\dot{\theta}$ becomes zero, the conservation equation becomes:

$$(I_1+\mu l^2+\mu r l \cos q)\dot{q}=h_0 \quad (20)$$

It is obvious that for larger $I_1+\mu l^2$, \dot{q} is smaller, and thus there is more time before the tail angle q reaches its limits. By integrating (22) one gets an implicit equation for q , which better describes the nature of the system's instability in terms of the tail drift:

$$(I_1+\mu l^2)q+\mu r l \sin q-(I_1+\mu l^2)q_0-\mu r l \sin q_0=h_0(t-t_0) \quad (21)$$

VI. SIMULATION RESULTS

A. Reaction Wheel – Tail Comparison

First, simulations were carried out using Matlab for a tail and a reaction wheel for body parameters $m_0=40kg$, and $I_0=2kgm^2$ (realistic values for a cheetah or a robot). Both appendages were hinged at distance $r=0.4m$ from the body's CoM, while constraints were considered for the length of the tail and the radius of the reaction wheel. We assumed that the tail's workspace was limited at the back of the robot, while the reaction wheel occupied the whole disk defined by its radius, occupying also a part of the body's space. Therefore, the tail's length could not be larger than the robot's height, while the wheel should have a small radius in order to occupy the least body space possible.

We simulated two cases: one with a reaction wheel of maximum possible radius $\rho=0.25m$, and one with a tail of

maximum possible length $l=0.5m$ (two times greater). We assumed that a reasonable change of the body pitch angle – considering no initial angular momentum – would be $\Delta\theta=10^\circ$, and a reasonable time interval would be almost equal to the cheetah's swing time $t=0.2s$, (see Table I). A suitable tail's mass $m_1=0.5kg$ was calculated using (14). In order to make a proper comparison, the two appendages should have equal MoI, and thus we considered the wheel's mass to be four times greater than the tail's mass, i.e. $m_1=2kg$, since wheel's MoI is given by $I_1=m\rho^2$. Simulation results are presented in Fig. 3.

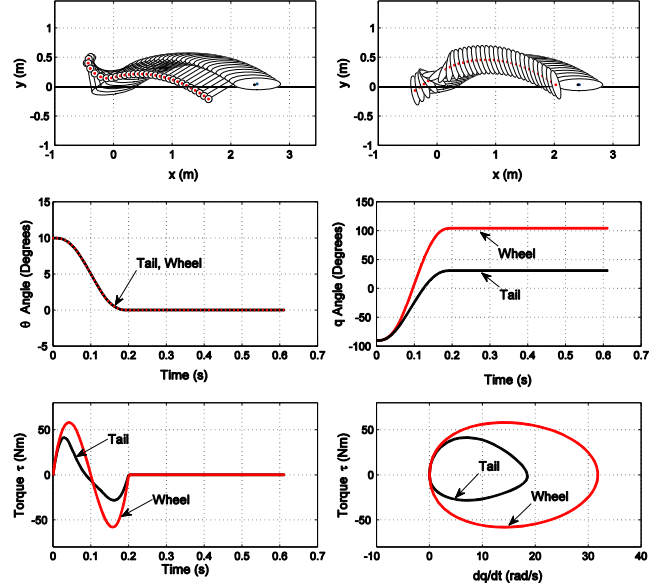


Figure 3. Simulation results for a $\Delta\theta=10^\circ$ maneuver with appendages of equal MoI. Red line: reaction wheel data, Black line: tail data.

Studying the simulation results presented in Fig. 3, we reach the following important conclusions:

a. The results reveal a symmetry for the wheel case, but not for the tail case; this is because the tail's CoM moves with respect to its hinge, while the wheel's CoM does not.

b. Less torque is required for the tail case; this is because a force appears at the joint (only in the tail case) creating an extra torque that helps the motor rotate the body.

c. The motor needs to run at a much higher speed in the wheel case; that is for the same result, more power is requested from the motor.

B. Comparison for Different Hinge Positions

Finally, we carried out simulations using the same parameters, varying the hinge position of the appendages. Figure 4 shows results for a reaction wheel and a tail, first hinged at the body's CoM, and then at a distance $r=0.4m$. Based on Fig.4, we reach the following conclusions:

a. For the tail case, much greater torque and motor speed are needed if the tail is hinged at the body's CoM. This is because, the force appearing at the hinge creates no extra torque, if the tail is hinged at the body's CoM; this torque could help the motor rotate the body using less torque.

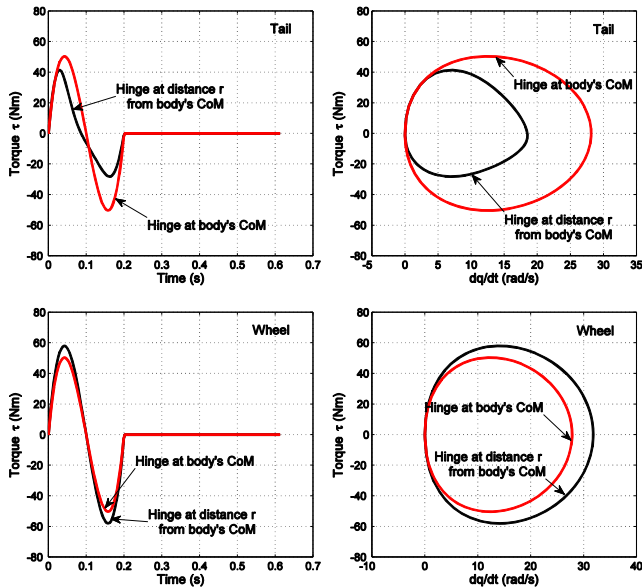


Figure 4. Simulation results for a $\Delta\theta=10^\circ$ maneuver for different hinge positions. First row: tail data, Second row: reaction wheel data, Red line: hinge at body's CoM, Black line: hinge at the edge.

b. For the wheel case, slightly greater torque and speed are needed if the reaction wheel is hinged at the edge; this is mainly due to the slight displacement of the system CoM with respect to the body's CoM, caused by the displacement of the wheel's hinge.

VII. CONCLUSION

In this work, we studied the attitude dynamics and the control of quadruped robots using tail-like appendages during the flight phases of a stride. Inspiration and data were first obtained from cheetah's fast galloping techniques. Second, a two-body template was introduced to describe the dynamics of a large body controlling its attitude with a rotating appendage. Several matters concerning the holonomy of the planar two body system and its implications on dynamics and attitude control were discussed in detail. By employing cyclic coordinates, all possible reductions were performed on the dynamics to finally lead to the design of model-based controllers, while basic steps and formulas were proposed for selecting the key parameters concerning the design of such systems. Finally, simulation results were presented regarding robot maneuvers using a reaction wheel and a tail, and useful conclusions were derived. As it was shown, when using a reaction wheel at a distance from the main body's CoM, greater torque and higher speed are requested from the motor, compared to these requested when a tail of the same MoI is used for the same maneuver.

REFERENCES

[1] Hickman, G. C., "The mammalian tail: a review of functions," *Mammal Review*, 9:143–157, 1979.
 [2] Alexander, R. McN. and Vernon, A., "The mechanics of hopping by kangaroos (Macropodidae)," *Journal of Zoology*, 177: 265-303, 1975.

[3] Lee DV, Bertram JE, Todhunter RJ, "Acceleration and balance in trotting dogs," *Journal of Experimental Biology* 202.24: 3565-3573, 1999.
 [4] Collins, S. H., Adamczyk, P. G., & Kuo, A. D., "Dynamic arm swinging in human walking," *Proceedings of the Royal Society B: Biological Sciences*, rspb20090664, 2009.
 [5] Zeglin, J. G., "Uniroo: A One Legged Dynamic Hopping Robot," Massachusetts Institute of Technology, Mechanical Engineering Department, 1991.
 [6] Takita, K.; Hodoshima, R., Hirose, S., "Fundamental mechanism of dinosaur-like robot TITRUS-II utilizing coupled drive," *Proceedings 2000 IEEE/RSJ Int. Conf. on Intelligent Robots and Systems*, vol.3, no., pp.1670,1675 vol.3, 2000.
 [7] Jusufi, A., et al. "Righting and turning in mid-air using appendage inertia: reptile tails, analytical models and bio-inspired robots," *Bioinspiration & biomimetics* 5.4: 045001, 2010.
 [8] Johnson, Aaron M., et al. "Tail assisted dynamic self-righting," *Proceedings of the Fifteenth Int. Conf. on Climbing and Walking Robots and the Support Technologies for Mobile Machines*, Baltimore, MD, USA, July 2012.
 [9] Kohut, N. J., et al. "Precise dynamic turning of a 10 cm legged robot on a low friction surface using a tail," (ICRA), *2013 IEEE Int. Conf. on Robotics and Automation*, 2013.
 [10] Fisher, C., and A. Patel. "Preparation of Papers for IFAC Conferences & Symposia: FlipBot: A Lizard Inspired Stunt Robot", 2014.
 [11] De, A., Johnson, A. M., & Koditschek, D. E., "Monopedal Hopping with a Leg and a Tail."
 [12] Mutka, A., Orsag, M., & Kovacic, Z., "Stabilizing a quadruped robot locomotion using a two degree of freedom tail," *IEEE 21st Mediterranean Conf. on Control & Automation*, 2013.
 [13] Berenguer, F. J., & Monasterio-Huelin, F. M., "Zappa, a quasi-passive biped walking robot with a tail: Modeling, behavior, and kinematic estimation using accelerometers," *IEEE Transactions on Industrial Electronics*, 55.9: 3281-3289, 2008.
 [14] Jensen-Segal, S., Virost, S., & Provancher, W. R., "ROCR: Dynamic vertical wall climbing with a pendular two-link mass-shifting robot," *IEEE Int. Conf. on Robotics and Automation*, 2008.
 [15] Papadopoulos, E., Fragkos, I., & Tortopidis, I., "On robot gymnastics planning with non - zero angular momentum," *IEEE Int. Conf. on Robotics and Automation*, 2007.
 [16] Xin, X., Mita, T., & Kaneda, M., "The posture control of a two-link free flying acrobot with initial angular momentum," *Automatic Control, IEEE Transactions on* 49.7: 1201-1206, 2004.
 [17] Reyhanoglu, M., & McClamroch, N. H., "Controllability and stabilizability of planar multibody systems with angular momentum preserving control torques," *American Control Conference, IEEE*, 1991.
 [18] Sadati, Nasser, et al., "Hybrid Control and Motion Planning of Dynamical Legged Locomotion," Vol. 2. John Wiley & Sons, 2012.
 [19] Briggs, Randall, et al., "Tails in biomimetic design: Analysis, simulation, and experiment," (IROS), *IEEE/RSJ Int. Conf. on Intelligent Robots and Systems*, 2012.
 [20] Chang-Siu, Evan Heng Seng. "A Tale of a Tail." UC Berkeley: Mechanical Engineering, 2013.
 [21] Cherouvim, N. and Papadopoulos, E., "Speed Control of Quadrupedal Bounding Using a Reaction Wheel," *Proc. 2006 IEEE Int. Conf. on Control Applications*, (CCA '06), October 4-6, 2006, Technische Universität München, Munich, Germany, pp. 2160-2165.
 [22] Casarez, C., Penskiy, I., & Bergbreiter, S., "Using an inertial tail for rapid turns on a miniature legged robot," *2013 IEEE Int. Conf. on Robotics and Automation*, 2013.
 [23] Schmidt-Wetekam, C., & Bewley, T., "An arm suspension mechanism for an underactuated single legged hopping robot," *IEEE Int. Conf. on Robotics and Automation*, 2011.
 [24] <http://spectrum.ieee.org/automaton/robotics/robotics-hardware/fast-running-biped-robot-based-on-velociraptor>
 [25] National Geographic's coverage of cheetahs in the magazine's November 2012. "Filming the World's Fastest Runner", <http://ngm.nationalgeographic.com/2012/11/cheetahs/behind-the-scenes-video>
 [26] Jazar, R. N., *Advanced dynamics: rigid body, multibody, and aerospace applications*. John Wiley & Sons, 2011
 [27] Bloch, A. M., *Nonholonomic mechanics and control* (Vol. 24). Springer Science & Business Media, 2003.